Biosensors and Bioelectronics 42 (2013) 447–452

Contents lists available at SciVerse ScienceDirect

Biosensors and Bioelectronics

journal homepage: www.elsevier.com/locate/bios

An integrated solution for rapid biosensing with robust linker free covalent binding surfaces

Yongbai Yin [a,*], Marcela M.M. Bilek [a], Keith Fisher [b], Chuan Guo [c], David R. McKenzie [a]

[a] School of Physics, University of Sydney, NSW 2006, Australia
[b] School of Chemistry, University of Sydney, NSW 2006, Australia
[c] School of Biochemical Engineering, University of Sydney, NSW 2006, Australia

ARTICLE INFO

Article history:
Received 27 September 2012
Received in revised form
13 November 2012
Accepted 14 November 2012
Available online 22 November 2012

Keywords:
Biosensors
Ellipsometry
Linker-free surfaces
Antigen–antibody reactions
Freeze-dry

ABSTRACT

A novel integrated biosensor methodology is proposed and demonstrated. The methodology utilizes a nitrogen-containing plasma polymer to achieve linker-free binding of a layer of biorecognition molecules. The sensor surface has been shown to maintain its performance after freeze-drying providing a long shelf life under ambient conditions. The sensor is configured for single wavelength ellipsometric detection providing a low cost, versatile, and rapid sensing and diagnosis platform suitable for a wide range of applications and end-users. The merits of the methodology are demonstrated using three antigen–antibody pairs.

1. Introduction

Biosensing using a biological recognition element is the preferred approach to identify and quantify biologically-relevant analytes. Suitable technology for sensing the attachment of biomolecules to a surface is currently one of the challenges to the widespread use of diagnostic array technologies in medicine and medical science research. The reliable and convenient detection of attachment of submonolayer amounts of molecules using label free technology will allow diagnostic arrays to be used in point of care medical applications and as a routine laboratory tool. Approaches that have been demonstrated using biological recognition elements include antigen–antibody interactions (Stayton et al., 1995; Lin et al., 1997), oligonucleotides (Schena et al., 1995; Southern et al., 1994), lectin–glycoprotein and hormone–receptor interactions (Lee et al., 1994; Kuno et al., 2005). In these interactions, molecular binding or detaching is quantified or sensed using a transducer. Proposed sensing techniques include scattering interferometry (Bornhop et al., 2007), microcantilevers (Shekhawat et al., 2006), electrical impedance spectrometry (Giaever and Keese, 1993), magnetic relaxation biosensing (Perez et al., 2002), and a variety of methods based on ellipsometry (Schuster et al., 1993; Jin et al., 1995). Currently all the techniques suffer from at least one of the following drawbacks: lengthy and complex processing for the preparation of linkers to provide robust immobilization of the initial biological recognition layer, non-specific interactions, a short shelf life of pre-prepared sensors, and the lack of a convenient, reliable and rapid diagnosis method (Wu et al., 2001; Olle et al., 2005). An integrated solution that brings together in the sensor design a simple and universal immobilization, adequate storage shelf life and simple sensing methodology is required before the technology is suitable ideally for the consumer market.

Covalent immobilization of the biomolecular recognition element is preferred over immobilization by physical interactions, as physically bound biomolecules can be detached during use and often are destabilized by the interactions that immobilize them on the surface. While physical immobilization is possible with textured surfaces such as nitrocellulose, experience with textured surfaces for antibody arrays shows that a large loading of antibodies is required in order to achieve the required density of accessible attached molecules. This leads to a requirement for 4–10 times the antibody loading than a flat surface (Mok and Li, 2008). Covalent binding is usually achieved by employing linker groups, which require specialized and complex chemical procedures to prepare them on the surface, and are often not able to retain the activity of the bound molecule over a practically useful time (Radadia et al., 2011; Fletcher et al., 2010; Zheng et al., 2011). A simple approach to covalent binding that is effective across a broad range of molecules has been recently developed

* Corresponding author.
E-mail address: yyin@physics.usyd.edu.au (Y. Yin).

0956-5663/$ - see front matter © 2012 Elsevier B.V. All rights reserved.
http://dx.doi.org/10.1016/j.bios.2012.11.015

(Bilek et al., 2011; Yin et al., 2009a, 2009b, 2009c; Yin et al., 2009a, 2010b). This approach relies on the deposition of a thin layer of nitrogen-containing plasma polymer (NPP) which delivers highly reactive radical species to the surface. These radicals covalently capture protein from solution to immobilize an almost fully dense monolayer of covalent bound protein. This approach has been demonstrated using a wide range of proteins and various analysis methodologies.

In this study, we integrate the covalent binding capacity into a complete biosensor methodology in which the recognition proteins are immobilized covalently, followed by freeze-drying to retain their activity during shelf storage. The readout technique we develop in this work is single wavelength, fixed incident angle ellipsometry (Arwin, 2001; Nirschl et al., 2010; Yin et al., 2011). We develop a sensor design that optimizes and linearize the shift in ellipsometric parameters. The advantage of this approach is that the end-users do not need to carry out complex sensor preparation which compromises repeatability and reliability.

2. Experimental section

2.1. Plasma polymer deposition

The plasma polymer deposition method and system was reported previously (Yin et al., 2009a). The schematic diagram of the system is given in the supporting information (Fig. S1(a) of SI). Briefly, the NPP deposition system included two powered electrodes: one radio frequency (RF) powered electrode at 13.56 MHz operated at 120 W to generate background plasma; the other was a substrate holder connected to a pulse voltage source at 200 V with pulse length 10μs and repetition 10 kHz to control the ion impact energy. Gases injected into the plasma chamber were acetylene (12 sccm), nitrogen (4 sccm), and argon (4 sccm). The pressure of the system was maintained at 20 Pa. During NPP deposition, the substrate temperature was not independently uncontrolled and was lower than approximately 60 °C.

2.2. Freeze-drying method for end-user ready biosensors

The procedure for freezing-drying adopted in this work is as follows: 2.5% sucrose in buffer was added prior to freezing to stabilize the immobilized proteins; the protein immobilized plasma polymer surfaces were rinsed and transferred to Falcon tubes containing 2.5% sucrose in PBS buffer, each tube contained one NPP biosensor with 2 ml of the sucrose containing buffer, then the tubes were placed in liquid nitrogen and the samples were frozen. Once frozen, the samples were transferred to a drying chamber (a Christ Alpha 2–4 LDplus freeze dryer) with 0.3 mbar pressure for 48 h until the drying process was completed. The samples were then stored in a desiccant with Sigma silica drying agent. The desiccated samples were stored at room temperature capped at 20 °C with a non-heating air conditioning during the autumn–winter seasons at Sydney, Australia (5–25 °C).

2.3. Materials and bio-assays

Proteins tested and chemicals used were all purchased from Sigma without further purification except human tropoelastin, including horseradish peroxidase (Cat no P6782), bovine liver catalase (Cat no C3155), calf skin collagen 1 (Cat no C9791), Microperoxidase-11 (Cat no M6756), BMP 7 (Cat no B1434), human serum IgG (Cat no I4506), anti-human IgG (Cat no I3266), protein-A (Cat no P1406), HRP antibody (Cat no P7899). Human (recombinant) tropoelastin corresponding to amino acid residues 27–724 of GenBank entry AAC98394 (gi 182020) was expressed and purified, tetramethylbenzidine (TMB, 3,3′,5,5′ tetramethylbenzidine, Cat no T0440), and anti-elastin (called anti-tropoelastin in the text)) clone BA-4 antibody (Cat no E4013).

The procedure for HRP attachment and activity analysis is as follows, unless specified in the text. Samples were incubated for 20 h in HRP (50 μg/ml) in 10 mM phosphate buffer (PB) at pH 7.0. Incubations were in 75 mm sterile Petri dishes with rocking. After the incubation, the samples were washed six times each for 20 min in 10 mM phosphate buffer pH 7.0. The first wash was performed in the Petri dish used for enzyme incubations. Then the samples were transferred to a clean Petri dish for the next five washes. Active HRP on the surfaces of the samples was measured by clamping the sample (approx 15×15 mm^2) between two stainless plates separated by an O-ring (inner diameter 8.0 mm, outer diameter 11.0 mm) that sealed the surface. The top plate contained a 5.0 mm diameter hole enabling the addition of 75 μl of the HRP enzyme substrate, TMB. After 30 s (or the duration specified in the text), 25 μl of reacted TMB was taken and added to 50 μl of 2 M hydrochloric acid to stop the reaction. A further 25 μl of unreacted TMB was then added to bring the volume to 100 μl. The absorbance of the solution at 450 nm was then measured using a Beckman DU530 Life Science UV/VIS spectrophotometer. All enzyme activity tests including rocking time were performed at 23 ± 1 °C. SDS cleaning in XPS analysis to remove physically immobilized proteins was carried out using 2% SDS in Milli-Q water and rocking for 4 h at 70 °C followed by rinsing in water for five times 5 min each. Sodium Dodecyl Sulfate (SDS) elution during the ellipsometry analysis was conducted at room temperature with the procedure specified in the text and supporting information.

2.4. Biosensor diagnosis methods

The NPP biosensors were characterized ellipsometrically using a J.A. Woollam M-2000 spectroscopic ellipsometer, which allows us to obtain spectral information covering a wide range of wavelengths, including at the principal detection wavelength at 632 nm. The ellipsometry system has a typically low sensitivity and high accuracy ($\pm 0.01^\circ$ for Psi). In this work the error bars we applied were 0.02° or 0.03° for Psi to represent the system errors of the detection with confidence. A flow cell with 70° incidence angle windows was used during the ellipsometry analysis. All ellipsometry analysis was done at 70° incident angle. Soaking for protein immobilization or interaction was all conducted for 30 min unless specified in the text. A photoelectron spectroscopy (XPS) system, (model: SPECS-XPS, from SPECS, Germany) was used to analyze the element concentration and binding energies of the plasma polymer surfaces. The XPS system was equipped with a high sensitivity PHOIBOS 150-9 MCD energy analyzer, capable of detecting medium sensitivity elements to a trace level in an order of 100 ppm. Al K-alpha X-ray source (1486.74 eV) was used in the analysis.

3. Results

3.1. Sensing optimization

The concept of our biosensor methodology using ellipsometry is illustrated in Fig. 1. In Fig. 1a, spectra for the ellipsometric parameter Psi are calculated for 3 example sensors with different thicknesses of the NPP layer on a 150 nm silicon nitride coated silicon wafer support. The sensors are assumed to be used in a water ambient with sensing light incident at an angle of 70°. The positions of the valleys in the spectra correspond to the wavelengths that give a pseudo-Brewster angle of 70°. The sensitivity, shown by the change in Psi caused by adding a 1.0 nm thick protein layer of refractive index of 1.46, is plotted in Fig. 1b. The sensitivity near the valley is

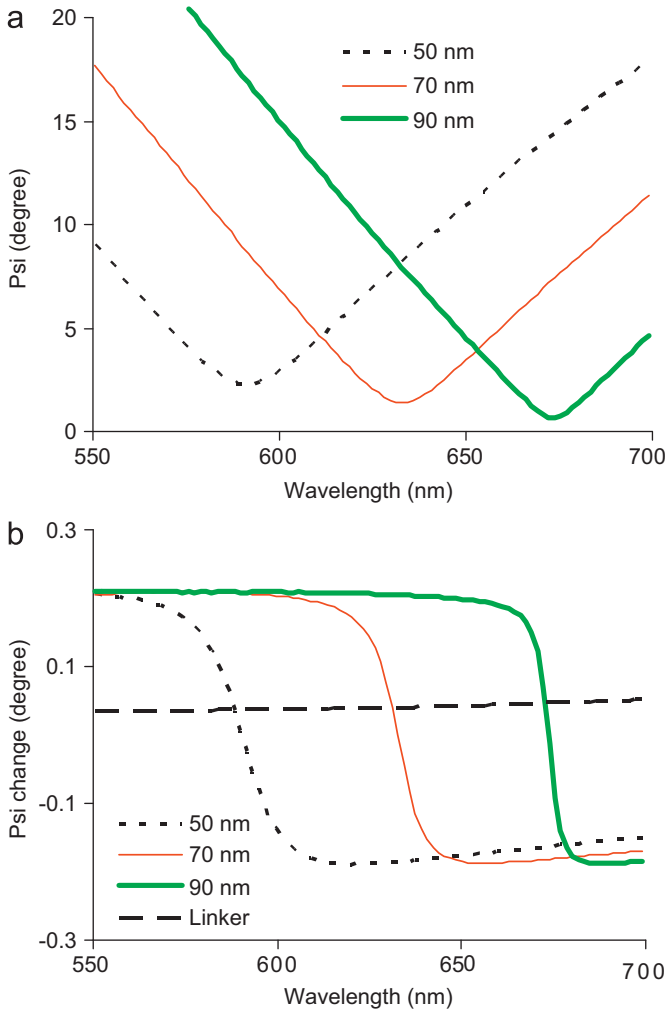

Fig. 1. (a) the ellipsometry spectra of Psi for sensors with different NPP layer thickness, (b) the sensitivity, or the change of Psi caused by the binding of a 1 nm thick protein layer, for the sensors in (a) as a function of wavelength, compared with a silicon sensor with an 1 nm thick self-assembled monolayer linker.

low and varies significantly with small changes in sensing wavelength; therefore, it is necessary to choose the NPP thickness to avoid locating the valley of the Psi spectrum near the 632 nm sensing wavelength. The sensitivity is high and stable for wavelengths that lie away from the valley. For comparison, the sensitivity (the change of Psi) of a conventional silicon sensor with a self-assembled monolayer linker layer of 1.0 nm thickness on silicon was also simulated (Fig. 1b). These results show that with an appropriately designed sensor structure, the sensitivity of our sensor can be made much higher than for a silicon sensor with a conventional self-assembled monolayer as an immobilization layer. Fig. S1(a) of SI shows the flow chart of the proposed biosensor methodology using the antigen–antibody interaction as an example. The steps are: design and construct a biosensor according to the principle shown in Fig. 1a and b with an NPP top layer; covalently immobilize antigen on the biosensor (as an immnosensor); carry out a freeze-drying treatment; store the freeze-dried sensors in dry air; and finally, when needed, use the sensor for diagnosis.

3.2. Linker-free covalent immobilization of proteins on plasma polymers

The covalent binding of the proteins to the surfaces was verified by its persistence when exposed to rigorous washing in SDS detergent. Techniques used for the covalent protein binding included ELISA, XPS, QCMD and ellipsometry. Proteins used in the analysis included human tropoelastin, bovine liver catalase, horseradish peroxidase, microperoxidase-11, bone morphogenic protein-7, calf collagen 1 and anti-human IgG. Table 1 summarizes the proteins used and the method adopted for a range of covalent binding studies together with the covalent binding coverage observed on the NPP surfaces. The reasons for the high covalent protein binding capacity of the NPP surfaces compared with the DLC surfaces were investigated further using electron paramagnetic resonance (EPR) spectroscopy. DLC surface has been previously proposed for biosensor applications (Hartl et al., 2004). The radical density of the DLC surfaces was found using EPR to be similar to that of the NPP surfaces. The lower covalent protein binding capacity of the DLC surfaces could result from their significantly lower radical mobility as suggested in the EPR analysis, which is consistent with the one-dimensional quantum well model in our theoretical simulation for the radical transportation and protein covalent binding enhancement (Fig. S12 of SI). The high covalent binding capacity for a variety of proteins on the NPP surfaces is therefore attributed to their high density of reactive and mobile radicals. The high coverage of the covalent or strong binding of the proteins on the NPP surfaces provides a straightforward and reliable platform for biosensor applications (Wink et al., 1997; Williams and Blanch, 1994; Bilek and McKenzie, 2010).

3.3. Freeze-drying effect on protein binding

In the freeze-drying treatment, sucrose was used in the last step as a stabilizer. Sucrose and other sugars have been used successfully to stabilize freeze-dried non-immobilized proteins (Carpenter et al., 1987; Buchinger et al., 2009) and linker layers (Xia et al., 2004) and to retain the activity of freeze-dried HRP immobilized on ion implantation treated polymers (Bes et al., 1995). Fig. 2a shows the activity as a function of the number of days of rocking in buffer for HRP immobilized on NPP surfaces before freeze-drying (FD-before), after freeze-drying (FD-after) and for HRP immobilized on silicon surfaces (Si) without freeze-drying. Immediately after freeze-drying, the HRP immobilized on NPP had a comparable activity to that before freeze-drying and much higher than its activity on silicon without freeze drying. After 5 and 10 days of rocking in buffer, the activity of the enzymes with and without freeze-drying on NPP was still high compared with the enzymes on silicon. The enhanced activity and the ability to withstand prolonged buffer rocking was attributed to covalent binding in a native conformation, implying that the freeze-drying process did not change the conformation status of the immobilized proteins on NPP significantly. This may be due to multipoint covalent attachment of HRP proteins on the NPP. It has been suggested that multipoint covalent binding can assist in maintaining conformation of immobilized proteins (Bes et al., 1995; Fernandez-Lafuente et al., 1995). In Fig. 2b, we show the activity of the immobilized HRP as a function of storage time

Table 1
Covalent binding capacity for a variety of proteins on NPP surfaces using different analysis methods.

Protein	Methodology	Covalent coverage (%)
Human tropoelastin	XPS, QCMD, ELISA	$\geq$75
Bovine liver catalase	XPS, QCMD, Ellipsometry	$\geq$75
Horseradish peroxidase	XPS, QCMD, Ellipsometry	$\geq$75
Microperoxidase-11	XPS	$\geq$80
Bone morphogenic protein-7	XPS	$\geq$75
Calf collagen 1	Ellipsometry, QCMD, XPS	$\geq$80
Anti-human IgG	XPS, Ellipsometry	$\geq$75

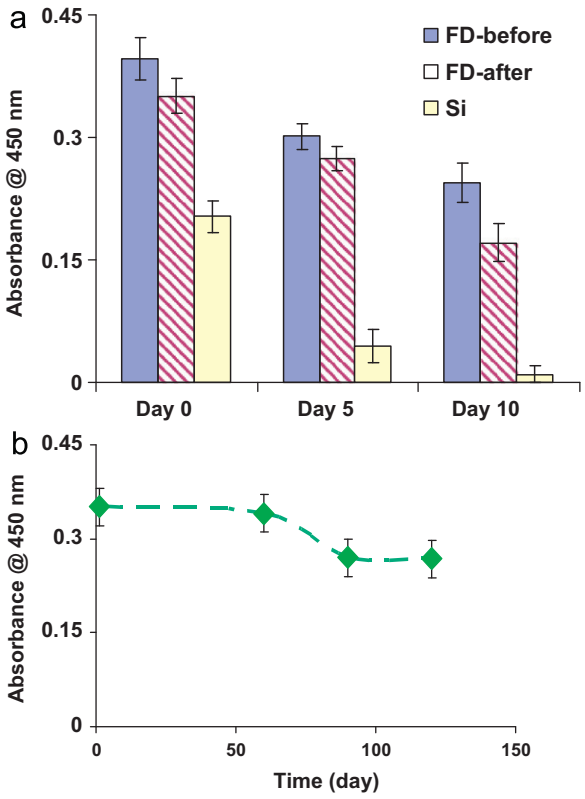

Fig. 2. The effect of freeze-drying on the conformation of the immobilized proteins and on protein binding strength: (a) the activity of immobilized HRP as a function of time in PB buffer for surfaces of silicon that had not been freeze-dried (Si), NPP that had not been freeze-dried (FD-before), and NPP with freeze-drying carried out after HRP immobilization (FD-after); (b) the retained activity of immobilized and freeze-dried HRP on NPP as a function of storage time after freeze-drying.

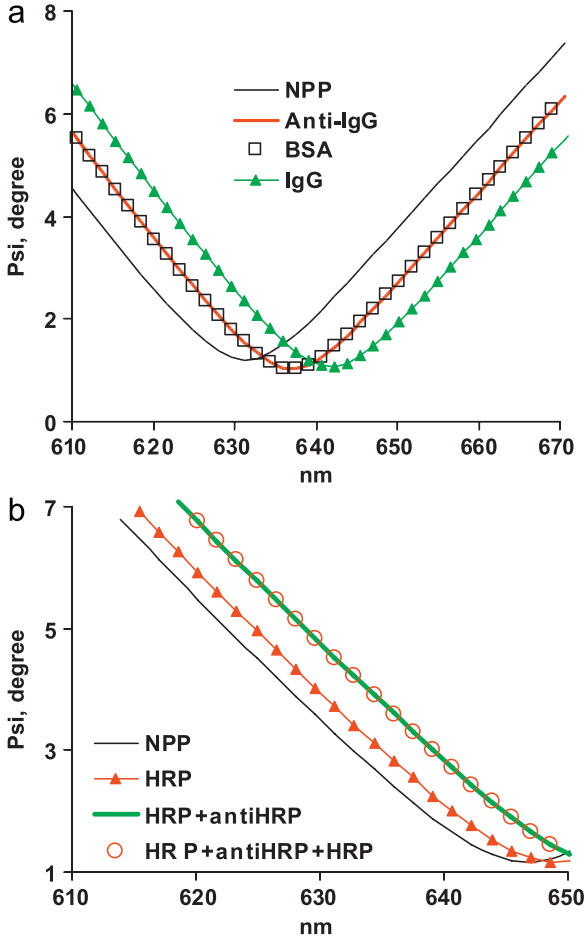

Fig. 3. Applications of the proposed biosensors for different antigen–antibody interactions, (a) ellipsometry spectra of Psi in the range near 632 nm for measured over the sequence of conditions: before protein immobilization on NPP (NPP), after incubation in 200 μg/ml anti-human IgG buffer followed by rinsing (Anti-IgG), followed by incubation in 1 mg/ml BSA solution (BSA), and then incubation in 200 μg/ml human antibody (IgG); (b) ellipsometry Psi spectra for biosensors before protein immobilization (NPP), after incubation in 50 μg/ml HRP buffer (HRP), followed by incubation in 4 μg/ml anti-HRP buffer (HRP+antiHRP); then further incubation in 100 μg/ml HRP buffer followed by rinsing (HRP+antiHRP+HRP).

after freeze drying. Storage was performed in a desiccator with ambient temperature in the range between 10 and 20 °C (Australia Sydney autumn–winter season, temperature capped at 20 °C using cooling-only air-conditioning). The result indicates that using the freeze-drying method, the enzyme immobilized NPP biosensors can be stored at room temperature under dry conditions for a long period of time, convenient for storage and transportation without refrigeration. If refrigerated storage is used, it is expected that an even longer lifetime of immobilized dried proteins is possible (Xia et al., 2004; Nosworthy et al., 2009). We also found that the freeze-drying did not alter the covalent binding nature of the proteins on the NPP surfaces, similar to those shown in Table 1 in SI without the freeze-drying treatment. This is expected as once a protein is covalently bound to a surface, it should be stable under conditions encountered in the freeze-drying treatment unless the surface itself is unstable. In contrast, in the case of silicon surfaces with self-assembled monolayer linkers, the silicon can gradually oxidize and release the bound self-assembled monolayer linker (Schlenoff et al., 1995; Mrksich et al., 1997).

3.4. *Nitrogen-containing plasma polymer biosensors without freeze-drying treatment*

The performance of the biosensors was first analyzed without introducing the freeze-drying treatment. In the following, we experimentally demonstrate the high sensitivity achievable with ellipsometry that was predicted theoretically above. Fig. 3 shows a range of protein interactions. Fig. 3a shows the measurements obtained over the sequence of operations: before protein immobilization, after incubation in 200 μg/ml anti-human IgG buffer solution and subsequent rinsing in buffer (Anti-IgG), followed by blocking in 1 mg/ml BSA and rinsing in buffer (BSA), then after soaking in 200 μg/ml human antibody and rinsing in buffer (IgG). The biosensor in Fig. 3a was constructed with an NPP layer thickness to place the spectral valley in Psi (the wavelength corresponding to the pseudo-Brewster angle of 70°) close to 632 nm. As shown in the discussion relating to Fig. 1a,b, the case where the minimum in Psi lies close to the sensing wavelength of 632 nm cannot be used for the biosensor readout because the sensitivity in this range is highly wavelength dependent. This means that this choice of NPP layer thickness is not appropriate for sensing with single wavelength ellipsometry at 632 nm. Note that the BSA blocking after anti-IgG immobilization did not introduce significant additional shifts. This is interpreted as the initial anti-IgG immobilization on the NPP surface resulting in a dense covalently bound monolayer.

Fig. 3b shows the Psi spectra for a correctly constructed biosensor for sensing at 632 nm. Fig. 3b shows measurements obtained over the sequence of operations: before protein immobilization (NPP), after incubation in 50 μg/ml HRP buffer and subsequent rinsing in buffer (HRP), followed by incubation in 4 μg/ml anti-HRP buffer and rinsing in buffer (HRP+antiHRP), and then further incubation in 100 μg/ml HRP buffer and rinsing in buffer (HRP+antiHRP+HRP). The resulting

changes in Psi are: hRP binding (0.43°), anti-HRP binding (0.80°), and no change for further HRP exposure. Since the typical angle sensitivity of a low cost ellipsometry system is better than 0.02°, this result shows that the NPP sensor provides a reliable analysis, because of the simple linear relationship between the immobilized protein layer thickness and the change of Psi. We calculate that the molecular ratio of the anti-HRP to initially bound HRP is 1:1.5. This indicates that the anti-HRP captured by the initial immobilized HRP also had a high density. Further incubation in HRP (to give the layer structure (HRP+antiHRP+HRP)) did not alter the reading. XPS analysis on the anti-HRP biosensor agreed reasonably well with the ellipsometry data in Fig. 3b which gave a value of 1.86 for the immobilized protein quantity ratio of the anti-HRP to the HRP using the shoulder in the C1s spectra near 288.5 eV for approximate quantification of immobilized proteins by using the method mentioned previously (Wagmer et al., 2002). The integrated intensity ratio in the range of the shoulder for the increment due to additional anti-HRP immobilization to that due to the HRP immobilization was 2.0, which was the approximately the same ratio as that obtained using the corresponding S 2p peaks in the XPS analysis. Considering the fact that in the XPS analysis, a thicker protein surface layer would be slightly over-counted due to the higher sensitivity for the top layer (Lubambo et al., 2006) unless only one monolayer layer of proteins is immobilized (Yin et al., 2010b), this is considered good agreement. More examples of biosensors can be found in SI (Fig. S9)

3.5. Freeze-dried nitrogen-containing plasma polymer biosensors

The sensitivity of the freeze-dried NPP biosensors using ellipsometric readout at 632 nm is shown in Fig. 4. Fig. 4a shows a NPP biosensor for human IgG measured over the sequence of operations: incubation in 20 μg/ml anti-IgG followed by freeze-drying (Anti-IgG+FD), incubation in 1 mg/ml BSA blocking (BSA), and the incubation in 10 μg/ml human IgG. After BSA blocking, the reaction with human IgG resulted in a change of Psi approximately 25 times larger than the change from the BSA blocking, demonstrating a high sensitivity of the NPP IgG biosensor.

In Fig.4b we show the operation of a freeze-dried protein-A biosensor. Protein-A is widely used in biosensors to orient antibodies (Muramatsu et al., 1987). The sequence of conditions at which measurements were taken was: protein-A immobilized and freeze-dried (PA+FD), 40 μg/ml anti-tropoelastin immobilization (Anti-tropo), 1 mg/ml BSA blocking (BSA), and 40 μg/ml human tropoelastin immobilization (Tropo). It shows that the freeze-dried biosensor with immobilized protein-A was functional to accommodate anti-tropoelastin for detecting tropoelastin. Combining with other protein-A immobilized biosensors using both ellipsometry and XPS (shown in Figs. S9c and S10c of SI) we found that approximately every two immobilized protein-A proteins can capture one antibody protein, giving approximately a 50% capture efficiency. Considering the larger size of an IgG compared to protein-A, this IgG capture efficiency of the immobilized protein-A is excellent, and it is consistent with the random model of protein adsorption and shows that almost all IgG molecules are correctly oriented.

The effectiveness of the freeze-drying was further analyzed using a NPP biosensor which was processed with protein-A immobilization and then human IgG soaking prior to the freeze-drying treatment. In Fig.4c, we show the response of the biosensor in the analysis with the sequence of operations: after protein-A and human IgG immobilization then freeze-drying treatment (PA+IgG+FD), 1 mg/ml BSA blocking (BSA), then 10 μg/ml anti-IgG immobilization (Anti-IgG). Such freeze-dried protein double-layer biosensors provide an opportunity for a wide range of end-users and applications and will have a particular advantage when rare antigen (or antibody) biosensors are required in medical diagnosis. More examples can be found in SI (see Fig. S10 in SI).

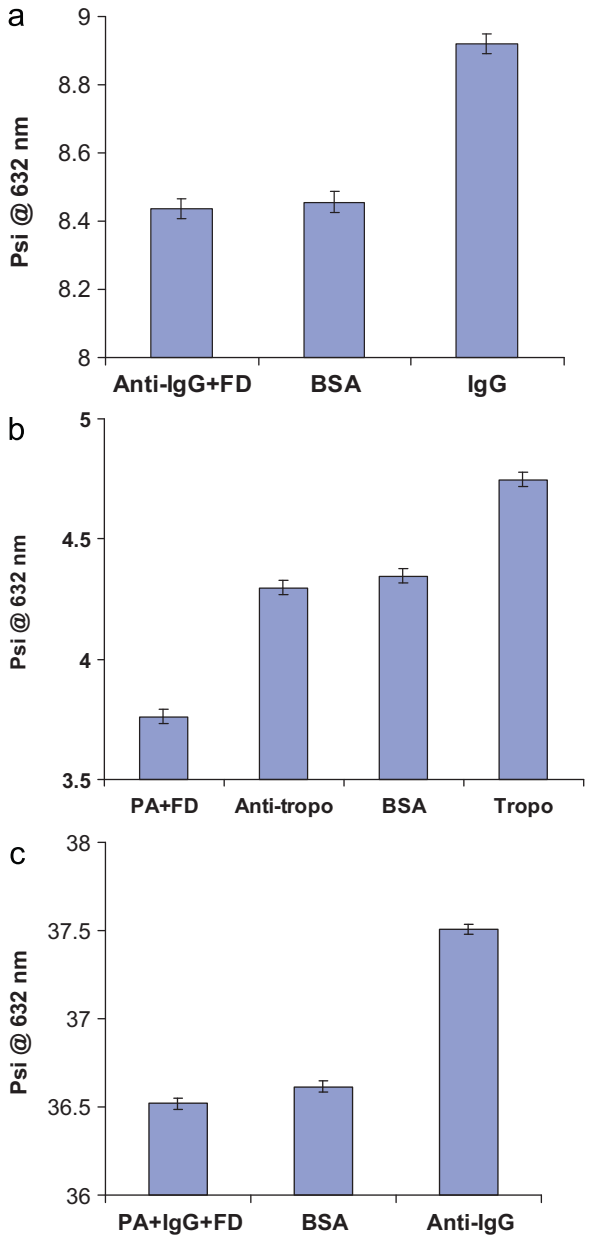

Fig. 4. Examples of biosensors with freeze-drying treatment using ellipsometry analysis, (a) a human IgG biosensor on anti-IgG immobilized biosensor with a sequence of after anti-IgG immobilization and freeze-dry (Anti-IgG+FD), BSA blocking (BSA), and human IgG immobilization; (b) a protein-A immobilized biosensor with a sequence of after protein-A immobilization and freeze-dry treatment (PA+FD), anti-tropoelastin immobilization (Anti-tropo), BSA blocking (BSA), and human tropoelastin immobilization (Tropo); (c) a protein-A then human IgG immobilized biosensor with a sequence of after protein-A and human IgG immobilization then freeze-dry treatment (PA+IgG+FD), BSA blocking (BSA), then anti-IgG immobilization (Anti-IgG).

4. Discussion and conclusions

We have demonstrated in this paper an integrated solution for biosensing. The methodology we have demonstrated is reliable, rapid, and easy to use. The reliability of the biosensors results from the high covalent binding capacity of the NPP surfaces for protein and the excellent performance of the biosensors after a freeze-drying treatment. The reliability is further ensured by the linear response that prevents small drifts in sensor properties during storage from changing the sensitivity. The rapidity and the end-user convenience are attributed to the optimized biosensor

optical design, the simplicity of the diagnosis method, and the simple storage procedure, enabling minimal involvement at the diagnosis step, especially for those not having specific biosensor formation facilities and skills. XPS and QCMD confirmed the covalent binding nature of the NPP surface before and after the freeze-drying treatment. The antigen–antibody interactions on the NPP biosensors were comprehensively reconfirmed after freeze-drying using the XPS technique. Three different pairs of antigen-antibodies, together with protein-A to accommodate different antibodies, were tested to demonstrate the new biosensor methodology. Using anti-HRP biosensors for consistency analysis, we found the ratio of sensing signal to BSA blocking signal was greater than 10, and the signal induced by BSA blocking was almost always within system errors with good repeatability from sample to sample (shown in Fig. S11 of SI).

The typical data collection time for ellipsometry analysis (single wavelength and single biological reaction step) for each biosensor is expected to be within a few minutes in most cases. This means in the biosensor applications the bottle-neck to limit the biosensor diagnosis throughput is not the data collection. Using the standardization of the NPP biosensors, a fast throughput of biosensor diagnosis can be achieved by rapidly rotating biosensors through a simple ellipsometry analysis unit while waiting for the biological reactions to run to completion. This can offer a convenient and low cost solution for matching the speed advantage of integrated diagnosis techniques such as imaging ellipsometry (Qi et al., 2010; Jin et al., 1996).

In summary, an integrated solution for a versatile biosensor technology has been demonstrated with the desirable features of long shelf life, simple storage procedure, reliable performance and minimal involvement of end-users. The technology combines the high protein covalent binding capacity of NPP surfaces with a high sensitivity, low cost diagnosis method that shows robust performance after freeze-drying. The covalent binding mechanism of the NPP surface was investigated by EPR spectroscopy. A model in which mobile electron spins are responsible for both the EPR signal and the covalent binding was confirmed. The merits of the technology were demonstrated experimentally using three antigen-antibody pairs.

Acknowledgments

We acknowledge financial support from Australian Research Council and provision of computing resources from APAC. We gratefully acknowledge technical discussion with Professors C.G. dos Remedios, J. Gooding, H.G.L. Coster and H. Yasuda, Drs W.R. Yang, D. Reilly, D. Bax, N. Nosworthy and T. Chilcott.

Appendix A. Supporting information

Supplementary data associated with this article can be found in the online version at http://dx.doi.org/10.1016/j.bios.2012.11.015.

References

Arwin, H., 2001. Sensors and Actuators 92, 43–51.
Bes, T., Gomez-Moreno, C., Guisan, J.M., Fernandez-Lafuente, R., 1995. Journal of Molecular Catalysis 98, 161–169.
Bilek, M.M.M., McKenzie, D.R., 2010. Biophysical Reviews 2, 55–65.
Bilek, M.M.M., Bax, D.V., Kondyurin, A., Yin, A., Nosworthy, N., Fisher, K., Waterhouse, A., Weiss, A.S., dos Remedios, C.G., McKenzie, D.R., 2011. Proceedings of the National Academy of Sciences 108, 14405–14410.
Bornhop, J., Latham, J.C., Kussrow, A., Markov, D.A., Jones, R.D., Sørensen, H.S., 2007. Science 317, 1732–1736.
Buchinger, S., Campen, E., Helmers, E., Morosow, V., Krefft, M., Reifferscheid, G., 2009. Cryobiology 58, 139–144.
Carpenter, J.F., Crowe, L.M., Crowe, J.H., 1987. Biochimica et Biophysica Acta—General Subjects 923, 109–115.
Fernandez-Lafuente, R., Cowan, D.A., Wood, A.N.P., 1995. Enzyme and Microbial Technology 17, 366–372.
Fletcher, S.J., Phillips, L.W., Milligan, A.S., Rodda, S.J., 2010. Biosensors and Bioelectronics 26, 1696–1700.
Giaever, I., Keese, C.R., 1993. Nature 366, 591–592.
Hartl, A., Schmich, E., Garrido, J.A., Hernando, J., Catharino, S.C.R., Walter, S., Feulner, P., Kromka, A., Steinmüller, D., Stutzmann, M., 2004. Nature Materials 3, 736–742.
Jin, G., Tengvall, P., Lundström, I., Arwin, H., 1995. Analytical Biochemistry 232, 69–72.
Jin, G., Jansson, R., Arwin, H., 1996. Review of Scientific Instruments 67, 2930–2936.
Kuno, A., Uchiyama, N., Koseki-Kuno, S., Ebe, Y., Takashima, S., Yamada, M., Hirabayashi, J., 2005. Nature Methods 2, 851–856.
Lee, J.W., Ryan, F., Swaffield, J.C., Johnston, S.A., Moore, D.D., 1994. Nature 374, 91–94.
Lin, V.S., Motesharei, K., Dancil, K.S., Sailor, M.J., Ghadiri, M.R., 1997. Science 278, 840–843.
Lubambo, A.F., Benelli, E.M., Klein, J., Schreiner, W., Camargo, P.C., 2006. Cell Biochemistry and Biophysics 44, 503–511.
Mok, W., Li, Y., 2008. Sensors 8, 7050–7084.
Mrksich, M., Dike, L.E., Tien, J., Ingber, D.E., Whitesides, G.M., 1997. Experimental Cell Research 235, 305–313.
Muramatsu, H., Dicks, J.M., Tamiya, E., Karube, I., 1987. Analytical Chemistry 59, 2760–2763.
Nirschl, M., Rantala, A., Tukkiniemi, K., Auer, S., Hellgren, A., Pitzer, D., Schreiter, M., Vikholm-Lundin, I., 2010. Sensors 10, 4180–4193.
Nosworthy, N.J., McKenzie, D.R., Bilek, M.M.M., 2009. Biomacromolecules 10, 2577–2583.
Olle, E.W., Messamore, J., Deogracias, M.P., McClintock, S.D., Anderson, T.D., Johnson, K.J., 2005. Experimental and Molecular Pathology 79, 206–209.
Perez, J.M., Josephson, L., O'Loughlin, T., Dagmar Högemann, D., Weissleder, R., 2002. Nature Biotechnology 20, 816–820.
Qi, C., Tian, X.S., Chen, S., Yan, J.H., Cao, Z., Tian, K.G., Gao, G.F., Jin, G., 2010. Biosensors and Bioelectronics 25, 1530–1534.
Radadia, A.D., Stavis, C.J., Carr, R., Zeng, H., King, W.P., Carlisle, J.A., Aksimentiev, A., Hamers, R.J., Bashir, R., 2011. Advanced Functional Materials 22, 1040–1050.
Schena, M., Schena, M., Shalon, D., Davis, R.W., Brown, P.O., 1995. Science 270, 467–470.
Schlenoff, J.B., Li, M., Ly, H., 1995. Journal of the American Chemical Society 117, 12528–12536.
Schuster, S.C., Swanson, R.V., Alex, L.A., Bourret, R.B., Simon, M.I., 1993. Nature 365, 343–347.
Shekhawat, G., Tark, S., Dravid, V.P., 2006. Science 311, 1592–1595.
Southern, E.M., Case-Green, S.C., Elder, J.K., Johson, M., Mir, K.U., Wang, L., Williams, J.C., 1994. Nucleic Acids Research 22, 1368–1373.
Stayton, P.S., Shimoboji, T., Long, C., Chilkoti, A., Ghen, G., Harris, J.M., Hoffman, A.S., S., 1995. Nature 378, 472–474.
Wagmer, M.S., McArthur, S.L., Shen, M., Horbett, T.A., Castner, D.G., 2002. Journal of Biomaterials Science, Polymer Edition 13, 407–428.
Williams, R.A., Blanch, H.W., 1994. Biosensors and Bioelectronics 9, 159–167.
Wink, T., van Zuilen, S.J., Bult, A., van Bennekom, W.P., 1997. Analyst 122, R43–R50.
Wu, G., Datar, H.D., Hansen, K.M., Thundat, T., Cote, R.J., Majumdar, A., 2001. Nature Biotechnology 19, 856–860.
Xia, N., Shumaker-Parry, J.S., Zareie, M.H., Campbell, C.T., Castner, D.G., 2004. Langmuir 20, 3710–3716.
Yin, Y., Nosworthy, N.J., Gong, B., Bax, D., Kondyurin, A., McKenzie, D.R., Bilek, M.M.M., 2009a. Plasma Processes and Polymer 6, 68–75.
Yin, Y., Wise, S.G., Nosworthy, N.J., Waterhouse, A., Bax, D., Youssef, H., Byrom, M.J., Bilek, M.M.M., McKenzie, D.R., Weiss, A.S., Ng, M.K.C., 2009b. Biomaterials 30, 1675–1681.
Yin, Y., Fisher, K., Nosworthy, N.J., Bax, D., Rubanov, S., Gong, B., Weiss, A.S., McKenzie, D.R., Bilek, M.M.M., 2009c. Plasma Processes and Polymer 6, 658–666.
Yin, Y., Bilek, M.M.M., McKenzie, D.R., 2010a. Plasma Processes and Polymers 7, 708–714.
Yin, Y., Bax, D., McKenzie, D.R., Bilek, M.M.M., 2010b. Applied Surface Science 256, 4984–4989.
Yin, Y., Nosworthy, N.J., McKenzie, D.R., Bilek, M.M.M., 2011. Thin Solid Films 519, 2968–2971.
Zheng, L., Xiong, L., Zheng, D., Li, Y., Liu, Q., Han, K., Liu, W., Tao, K., Yang, S., Xia, J., 2011. Talanta 85, 43–48.